Heat Mass Transfer (2009) 45:1083–1097
DOI 10.1007/s00231-009-0480-2

ORIGINAL PAPER

Buoyancy and cross flow effects on heat transfer of multiple impinging slot air jets cooling a flat plate at different orientations

S. A. Nada

Received: 23 April 2008 / Accepted: 28 January 2009 / Published online: 13 February 2009

Abstract The present article reports on heat transfer characteristics associated with multiple laminar impinging air jet cooling a hot flat plat at different orientations. The work aims to study the interactions of the effects of cross flow, buoyancy induced flow, orientation of the hot surface with respect to gravity, Reynolds numbers and Rayleigh numbers on heat transfer characteristics. Experiments have been carried out for different values of jet Reynolds number, Rayleigh number and cross flow strength and at different orientations of the air jet with respect to the target hot plate. In general, the effective cooling of the plate has been observed to be increased with increasing Reynolds number and Rayleigh number. The results concluded that the hot surface orientation is important for optimum performance in practical applications. It was found that for $Re \geq 400$ and $Ra \geq 10{,}000$ (these ranges give $0.0142 \leq Ri \leq 1.59$ the Nusselt number is independent on the hot surface orientation. However, for $Re \leq 300$ and $Ra \geq 100{,}000$ (these ranges give $1.59 \leq Ri \leq 42.85$): (i) the Nusselt number for horizontal orientation with hot surface facing down is less that that of vertical orientation and that of horizontal orientation with hot surface facing up, and (ii) the Nusselt number of vertical orientation is approximately the same as that of horizontal orientation with hot surface facing up. For all surfaces orientations and for the entire ranges of Re and Ra, it was found that increasing the cross flow strength decreases the effective cooling of the surface.

S. A. Nada (✉)
Department of Mechanical Engineering Technology,
High Institute of Technology, Benha University, Benha, Egypt
e-mail: samehnadar@yahoo.com

List of symbols

A	Area of the hot target surface, m^2
A_j	Area of j the enclosure side wall, m^2
B	Slot width, m
F	View factor
G	Irradiations, W/m^2
Gr	Grashof number
g	Gravity acceleration, m/s^2
H	Separation distance, m
h	Average heat transfer coefficient, W/m^2 K
I	Electric current, Amp.
J	Radiosity, W/m^2
k_a	Thermal conductivity of air, W/m K
k_g	Thermal conductivity of fiberglass, W/m K
k_w	Thermal conductivity of plexigalss enclosure wall, W/m K
Nu	Average Nusselt number
Pr	Prandtl number
q	Convection heat transfer rate, W
q_c	Conduction heat transfer rate, W
q_r	Radiation heat transfer rate, W
Ra	Rayleigh number
Re	Air Reynolds number
Ri	Richardson number
T_H	Hot surface temperature, K
T_j	Jet inlet temperature, K
T_w	Wall surface temperature, K
t_g	Thickness of fiberglass insulation, m
t_w	Thickness of plexiglass wall, m
V	Voltage input, volt
Vj	Jet exit velocity, m/s
α	Thermal diffusivity, m^2/s
β	Coefficient of volumetric expansion, 1/K
ε	Emissivity, dimensionless
ν	Kinematic viscosity, m^2/s

ρ Density, kg/m^3
σ Stefan–Boltzmann constant, W/m^2 K^4

1 Introduction

A single or multiple impinging fluid jet(s) incident normally on a surface is an effective heat transfer enhancement technique used in a wide range of engineering applications. Impinging fluid jets are used to heat, cool or dry surfaces in many industrial applications such as tempering of glasses drying of paper and textiles and cooling of metal sheets, turbine blades and electronic equipments. A single impinging fluid jet is often used to enhance and control heat transfer rate of a local area of a surface (area under the jet directly). Although such single jet provides very high heat transfer rate at the impinging zone, the heat transfer rate rapidly drops away from this zone. To obtain a uniform high heat transfer rate all over the surface a multiple or an array of jets are commonly used. In a slot jets array impinging a surface, a wall jet is formed downstream the impinging point of each jet. The interaction of each wall jet with that of the upstream jet results in the formation of vortices between the two jets. These vortices enhance the rate of heat transfer. At the same time, each jet is deflected by the cross flow coming from the upstream jets. This cross flow affects the heat transfer rate at the jets stagnation zones.

The effects of the cross flow and the vortices formed between adjacent jets on fluid flow and heat transfer characteristics have been studied for turbulent jets by many investigators. Sezai and Aldabbagh [1] investigated the effect of jet-to-jet spacing on the cooling rate of a surface. The study was carried out for different values of jet-to-jet spacing at a fixed separation distance between the jet orifice and the impingement plate. They noticed strong periodic oscillation in the stream wise profile of Nusselt number. The amplitude of these oscillations increased as the jet-to-jet spacing increased. A secondary peak in the Nusselt number profile was predicted between each two successive jets as a result of the interaction of their wall jets. Later, Sezai and Aldabbagh [2] investigated the flow and heat transfer characteristics of inline jet arrays for different jet-to-jet spaces and different nozzle to plate distances. They also noticed the formation of a secondary peak in the Nusselt number between each two jets. They showed that the superimposition of the secondary peak distorts the periodic Nusselt number profile. Other several numerical investigations have been carried out to study the cross flow effect on jet cooling [3–8]. All of these investigations showed the vortices formation between the adjacent jets. On the other hand, studies in jets in cross flow have shown that cross flow results in a decrease of heat transfer rate [9–15] at the jet impinging point. Goldstein and Behbahani [9] reported measurements for local heat transfer to an impinging air jet with and without cross flow. They reported that at large jet-to-plate spacing cross flow diminishes the peak heat transfer coefficient and at a smaller spacing cross flow can increase the peak heat transfer coefficient. Al-Sanea [10] reported that cross flow can reduce the Nusselt number by 60%. Metzger et al. [11] and Florschuetz et al. [12] measured the effect of cross flow on the average heat transfer in an array of round jets. They concluded that increasing cross flow strength decreases the heat transfer performance. Yoon et al. [13] reported that cross-flow formed by the spent air from the impinging jets should be avoided whenever possible because of its adverse effect on impingement heat transfer. On the other hand, Kanokjaruvijit and Martinez-boats [14] reported that impingement on dimpled surfaces performed best with maximum cross flow scheme and larger jet-to-jet spacing due to the coupled effect of impingement and channel flow. Yang and Wang [15] also reported that heat transfer enhancement of an inclined jet with cross flow can be found over wider span-wise region as the velocity ratio of jet to cross flow is increased. Aldabbagh et al. [16] numerically investigated flow and heat transfer characteristics of an impinging laminar square jet through cross-flow. They noticed the formation of the vortices between the adjacent jets. They concluded that the location, number and strength of these vortices depend on the jet to cross flow velocity and on the jet to plate spacing. Rady and Arquis [17] studied, numerically, heat transfer and fluid flow characteristics during laminar impinging slot jets cooling of a flat plate with symmetrical exhaust ports in the confinement surfaces. They showed that the confinement surface protrusion reduces the interaction between jet inlet and exhaust flow and enhances heat transfer rates.

Although most of jet impinging applications are turbulent, laminar jets are also encountered in many industrial applications such as microelectronic devices miniature geometry and jets of highly viscous fluid. Most of the published studies on jet impingement cooling considered forced convection heat transfer mode. In these studies the Buoyancy effect was neglected. The Buoyancy effect can be neglected for turbulent flow (High Reynolds number), however it can not be neglected for low Reynolds number laminar flow. For laminar jets flow (Low Reynolds number), the heat transfer mode in impinging jet region may fall in the natural, forced or mixed convection regimes depending on the relative strengths of the inertia/viscous forces and the buoyancy forces involved. The parameter that defines the convection regimes is the Richardson number, Ri ($Ri = Gr/Re^2$). In parallel, internal or external flow (flow parallel to the surface that confined it) the forced convection mode is dominant if $Ri \ll 1$, whereas the natural convection mode is dominant when $Ri \gg 1$. If Ri is of order of 1, then both forced and natural convection are comparable and the resulting heat transfer mode falls into mixed convection regime. In many applications of laminar jet impinging, the Buoyancy effect may be significant and the mixed convection mode must be considered for heat transfer analysis. The interaction between the buoyancy driven flow and the shear driven flow in jet impinging flow makes the resulting fluid flow and heat transfer process very complex. The process becomes more complicated in case of using multiple jets array. In this case the buoyancy driven flow, the jet walls interaction phenomenon, the vortices formed between adjacent jets and cross flow formed by the upstream jets affect each other in coupled manners.

Very limited published studies considered buoyancy effect in confined single slot jet impinging on a flat surface. Satuanarayana and Jaluria [18] studied buoyancy effect on laminar single slot air jet impinging on inclined surface. They found that the downward flow penetration increases with increasing flow inclination, decreasing jet exit buoyancy and increasing flow rate. They reported that when the spent air flow is discharged at a downward inclination in a laminar slot jet, the jet would eventually have a flow reversal if the exit buoyancy were sufficiently large. Yuan et al. [19] reported that buoyancy affects local wall friction and heat transfer for an impinging jet. More recently, Sahoo and Sharif [20] investigated the associated heat transfer in the mixed convection regime in the case of single slot jet impinging cooling of a constant heat flux surface. They reported that the average Nusselt number does not change significantly with Richardson number indicating that the buoyancy effects are not very significant on the overall heat transfer process for the range of the jet Reynold number considered in his study. Rady [21] carried out numerical experiments to investigate the effects of buoyancy on flow and heat transfer characteristics of a semi-confined laminar single slot jet impinging on an isothermal wall. Rady concluded that the interaction between the main flow and buoyancy induced flow results in developing local peaks in the Nusselt number towards the plate end. He reported that, for down wards facing (buoyancy assisted) flow the number of heat transfer peaks, the stagnation and the average number of the Nusselt number increase with the increase of the Richardson and Reynolds and the opposite was true for upward facing (buoyancy retarded) flow.

To the authors' knowledge, studies on buoyancy effect on heat transfer and fluid flow characteristics in multiple laminar jets impingement from jet arrays on surfaces are not available yet in the literature. Interactions of buoyancy, vortices and cross flow effects on heat transfer and fluid flow characteristics in multiple laminar jets impingement are also have not studied yet. Therefore, in the present study experimental investigations of the effects of buoyancy and cross flow on heat transfer characteristics of semi-confined laminar slot jet arrays impinging on a flat wall placed at different orientations are presented. The parameters studied include jet Reynolds number, Rayleigh number, Richardson number, strength of cross flow and orientation of the plate with respect to gravity. To study the buoyancy effects and its interaction with cross flow and vortices effects, the experiments were carried out for different orientations of the hot surface; namely: (1) vertical orientation, (2) horizontal orientation with hot surface facing down and (3) horizontal orientation with hot surface facing up. In the three cases of surface orientation s the jet flow is incident normally on the hot surface. To study the cross flow effect, the experiments of each orientation were carried out for two different directions of venting the spent flow: (i) spent flow venting with maximum cross flow, and (ii) spent flow venting with minimum cross flow. Figure 1 shows the experiments matrix of the hot surface orientations and spent flow venting directions.

2 Experimental setup and procedure

2.1 Experimental setup

A schematic diagram of the experimental setup is shown in Fig. 2. It consists of three sections: supply air duct, air plenum, and test section. The supply air duct was a 200 mm square duct and had an overall length of 1,500 mm. Air was forced through the duct using upstream variable speed centrifugal fan. The fan was connected to the diverging section of the air duct through a flexible section to avoid noise and vibration of the duct. The air flow rate was measured using an orifice flow meter with a digital manometer across the orifice. The orifice flow meter was calibrated using a laminar flow element with an accuracy of ±2%. The air duct was connected from the other side to the air plenum through a sealed fastened system. The air enters the plenum and passes through a honeycomp and a turbulence eliminating screen to straighten the flow and produce uniform velocity profile at the slots exit. The jet plenum was a 10-mm thick Plexiglass airtight box with outside dimensions 600 × 350 × 350 mm. An array of slots (sharp edges slots) of lengths 200 mm and widths 7 mm was opened in one side wall of the jet plenum with a spacing of 35 mm between each two adjacent slots. The plenum was supported on a stand through an axel to enable rotating the plenum around this axis to obtain different jet flow directions with respect to gravity.

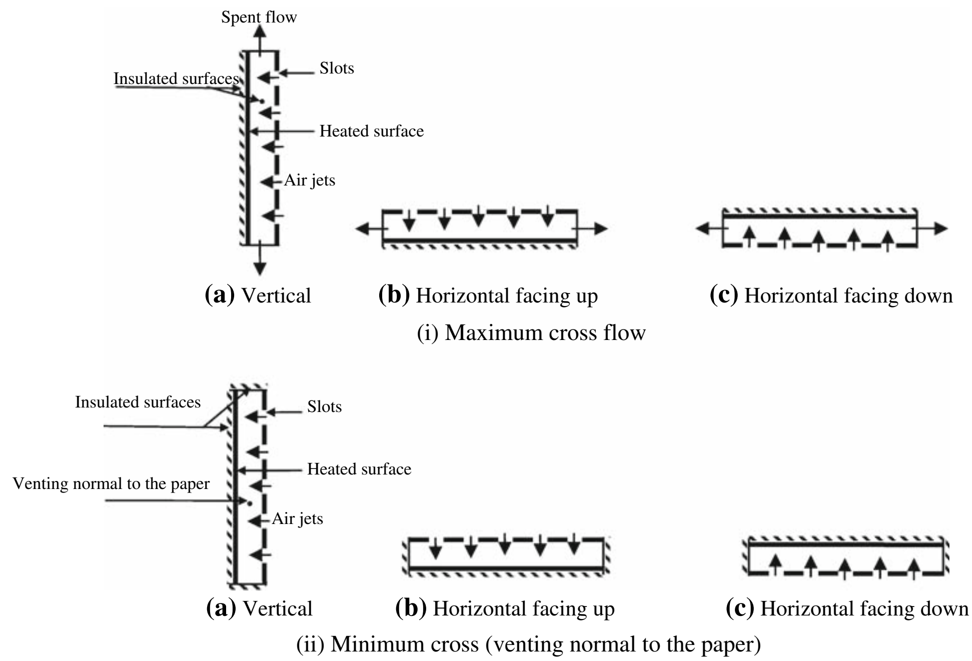

Fig. 1 Different arrangements of hot surface orientation and spent flow venting directions

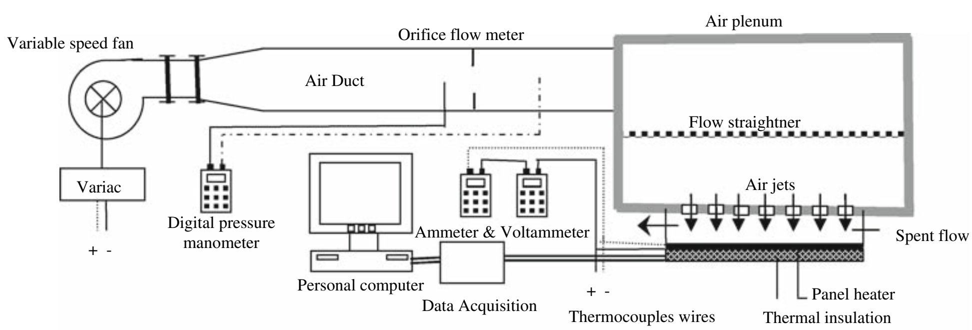

Fig. 2 Schematic diagram of the experimental set up

The test section (heated target plat) consists of a 350 × 200 mm nickel–chrome wire panel heater (1,000 W). The heater was made of nickel-chrome wire wound a round a thin mica plate and insulated from all sides with mica sheets covered by a thin copper sheet. The heater was connected with a DC power supply to control the power input to the heater. Voltage and current supplied to the heater were measured by digital voltmeter and ammeter of accuracy 0.025%. The heater was mounted inside a box having internal dimensions ($a \times b \times H$) 350 × 200 × 40 mm. The heater was mounted on the bottom wall of the box. The box was open from the top. The bottom and side walls of the box were made of double walls 10-mm thick Plexiglass sheet with 50-mm thick fiberglass thermal insulation inserted between the two walls as shown in Fig. 3a. The top edges of the box were fixed on the wall of the plenum box that contains the slots as shown in Figs. 2 and 3a. To carry out the experiments with maximum cross flow, the 200 × 40 mm two sides walls of the box were removed to vent the spent flow (see Fig. 2) and to carry out the experiments with minimum cross flow, the 320 × 40 mm two side walls of the box were removed to vent the spent flow.

The surface temperature distribution of the target plate was measured using 21 Teflon coated thermocouples (type T) distributed equally spaced on plate as shown in Fig. 3b. To facilitate the installation of the thermocouples without disturb the air convection currents, holes were drilled from the backside of the box bottom passing through the double walls, the heater and its copper cover plate. The thermocouples were inserted from these holes. The thermocouples junctions were fixed on the top surface of heated target plate as shown in Fig. 3a. To estimate conduction heat losses across the box walls, two thermocouples (type T) were fixed on the inner and outer surfaces (at the center) of each blind wall of the box. The temperature of air jet was measured by a thermocouple fixed inside the jet plenum. All thermocouples were calibrated in a constant temperature path and a measurement accuracy of ±0.2°C was

Fig. 3 Views of the test section and thermocouples distribution on target plate

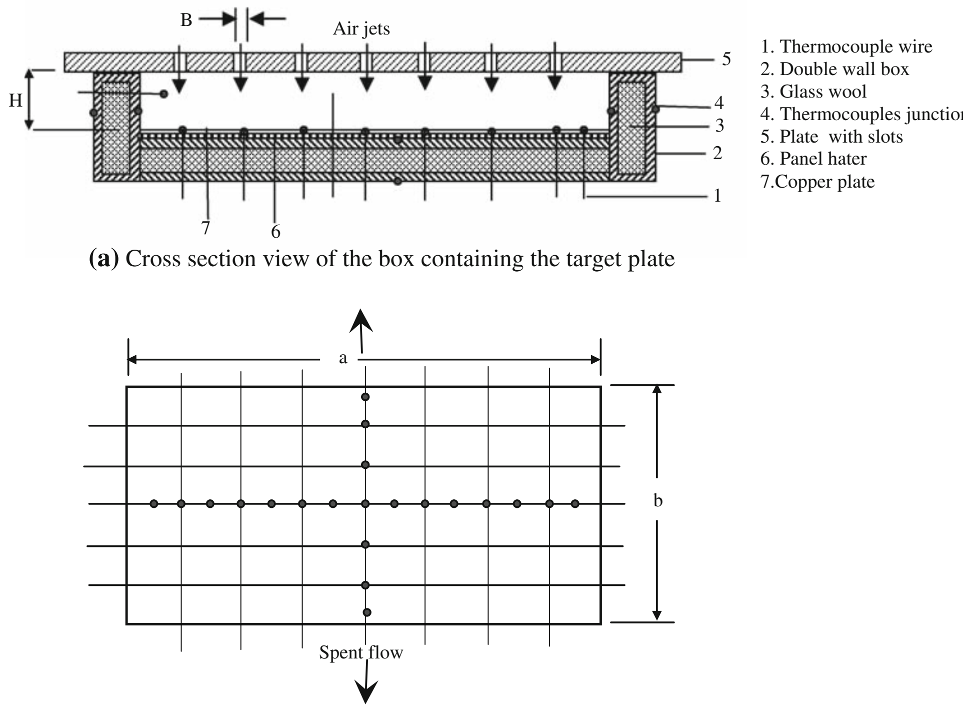

(a) Cross section view of the box containing the target plate

(b) Top view of target plate showing the thermocouples distribution

obtained. All the temperature signals were acquired using a data acquisition system and sent to a PC for data recording.

2.2 Experimental conditions

The ranges of the tested parameters in this study were:

Air Reynolds number (*Re*) based on (2*B*)	100–1,000
Rayleigh number (*Ra*) based on separation distance (*H*)	10,000–300,000
Slot width (*B*)	7 mm
Separation distance (*H*)	40 mm
Hot surface orientation	Vertical, horizontal facing up, and horizontal facing down
Direction of venting spent flow	Venting with maximum cross flow and venting with minimum cross flow.

2.3 Experimental procedure and program

The procedure and experimental program were as follow:

1. Adjust the target plate orientation to one of the tested orientations.
2. Remove the specified side walls of the box to obtain a specified venting direction of the spent flow.
3. Adjust the air fan speed to obtain a specified air flow rate and Reynolds number and allow the air jets to impinge the target surfaces.
4. Supply and adjust power to the heater to obtain a certain target surface temperature and Rayleigh number.
5. Wait until steady state condition was achieved.
6. Record all instruments readings (voltage, current, pressure and temperatures).
7. Repeat steps 4–6 for different values of *Ra* in the studied range.
8. Repeat steps 3–7 for different values of *Re* (100, 200, 300, 400, 500, 1,000).
9. Repeat steps 2–8 for the different venting directions of the spent flow.
10. Repeat steps 1–9 for the different orientations of the target plate.

2.4 Data reduction

The Rayleigh number (*Ra*) and the jet Reynolds number (*Re*) were calculated from the measured quantities as follows:

$$Ra = \frac{g\beta(T_H - T_j)H^3}{\alpha \nu} = Gr\,Pr \tag{1}$$

$$Re = V_j(2B/\nu) \tag{2}$$

where T_H is the average temperature of the target hot surface, V_j is the air jet velocity at the slot exit, T_j is the temperature of the air jet at the slot exit, H is separation distance between the slot orifice plate and the target hot surface, $2B$ is the hydraulic diameter (neglecting the slot width with respect to slot length) of the orifice jet, g is the acceleration of gravity and β, ν and α are the coefficient of volumetric expansion, kinematics viscosity, and thermal diffusivity of air, respectively. All air properties in Eqs. (1–2) were taken at $(T_H + T_j)/2$.

The Richardson number is calculated from

$$Ri = Gr/Re^2 \tag{3}$$

The energy balance for the box containing the heater gives

$$VI = q + q_C + q_r \tag{4}$$

where I and V are the electric current and voltage input to the heater, q is the heat transfer by convection from the hot target plate to the air jet, q_c is the heat losses by conduction through enclosure walls and q_r is the heat transfer by radiation from the box internal blind side walls and from the target hot plate to the box open sides. The conduction heat loss from the box is the sum of the conduction heat losses through the blind side walls and bottom wall of the box. The conduction heat losses can be calculated from

$$q_c = \frac{1}{(2t_w/k_w + t_g/k_g)} \sum A_j \Delta T_j \tag{5}$$

where j is the wall identification number, A_j is the area of the j side wall of the box, ΔT_j is the temperature difference between the inner and outer surfaces of the jth wall of the box, k_w is the thermal conductivity of the Plexiglas, t_w is the thickness of the Plexiglas wall, k_g is the thermal conductivity of the fiberglass insulation inserted between the box double walls and t_g is the thickness of the fiberglass insulation, respectively.

The radiation was incorporated in the losses based on the radiosity/irradiation formulation. All interior surfaces of the box were assumed to be opaque, diffuse, isothermal and gray. The radiation heat loss q_r from the box internal hot surfaces (blind sides and bottom surface) is the net rate at which radiation is incident on the open surfaces of the box. Identifying the box internal hot surfaces by the number j, the net rate at which radiation is incident on the box open surfaces is calculated from

$$q_r = \sum e_o A_o (sT_o^4 - G_o) \tag{6}$$

where the irradiation G_o is given by

$$G_o = \sum_{j=1}^{3} F_{oj} J_j \tag{7}$$

where F_{oj} is the view factor between the box open surface and the jth surface of the enclosure and J_j is the radiosity of that surface. J_j is given by

$$J_j = \varepsilon_j \sigma T_j^4 + (1 - \varepsilon_j) \sum_{i=1}^{5} F_{ji} J_i \tag{8}$$

The view factors F_{ij} between parallel and perpendicular surfaces were calculated based on the graphs and expressions given in Incropera and DeWitt [22] and Suryanarayana [23]. Equations 6–8 were solved together to find the radiation heat losses in terms of the surfaces temperatures of the box inside walls. In all experiments, the conduction heat losses through the enclosure walls and the radiation heat transfer to the open surfaces were within 4% and 10% of the input power, respectively.

The average heat transfer coefficient between the hot target plate and the air jet is given by

$$\bar{h} = \frac{q}{A(T_H - T_j)} \tag{9}$$

where A is the area of the target plate, T_H is the average temperature of the target plate (taken as the average of the readings of all thermocouples mounted on the target plate) and T_j is the temperature of the air jet. Temperature measurements showed that the variation of the surface temperature distribution on the target hot plate was within 1.5°C. This achieved uniform surface temperature is attributed to the high thermal conductivity of the target plate (copper). The effects of the different parameters (*Re, Ra, Ri, orientation of the target plate and the direction of air venting*) on flow behavior and heat transfer between the target plate and the air jet is reflected as an increase or decrease in T_H.

In most of the previous studies on turbulent air jet or laminar air jets, the dimensionless heat transfer coefficient Nu has been calculated based on slot width B [1, 2, 8, 10, 16, 21]. In consistent with these studies, the characteristics length B is used in the present study in calculating the Nusselt number as follows:

$$Nu = hB/k_a \tag{10}$$

where k_a is the thermal conductivity of the air taken at $(T_H + T_j/2)$.

Combining Eqs. 2–10 together, the expression of Nu can be put on the form

$$Nu = f(x_1, x_2, \ldots x_n) \tag{11}$$

where x_1 to x_n are all the variables that affect the experimental determination of Nu such as *I, V, T, H, k,* and ε as shown in Eqs. 2–10. The uncertainty ΔNu in the value of Nu was estimated based on the procedure of Holman and Gajda [24] and is expressed as follows

$$\Delta Nu = \sqrt{\sum_{i=1}^{n}\left(\frac{\partial Nu}{\partial x_i}\Delta x_i\right)^2} \qquad (12)$$

where Δx_i is the uncertainty in the x_i variable. The uncertainty in the various variables used in the determination of the Nusselt number were: 0.25% for the electric current I, 0.25% for the electric volt V, 0.2°C for any temperature measurement, 0.001 m for any distance value, 0.5% for the thermal conductivity of air, 2% for the thermal conductivities of Plexiglass and glass wool, and 5% for the emittance of the base plate and the plexiglass. It was found that the uncertainty (for all data) of Nu ranges from 5 to 8%.

3 Results and discussion

The experimental work was performed to study the effects of *Re, Ra,* orientation of the target hot surface and direction of venting the spent air on heat transfer rate from the target plate. The experiments were also conducted to study the interactions of buoyancy effect, cross flow effect, and vortices formation effect on each other. For each hot surface orientation and direction of spent flow venting, the heat transfer coefficient was obtained for different Rayleigh and Reynolds numbers. The average Nusselt number was found to be dependent on surface orientation, direction of venting the spent air, Rayleigh number and Reynolds number. Figures 4, 5, 6, 7, 8, 9, 10 show the variation of the average Nusselt number with Rayleigh number at various Reynolds numbers, target hot surface orientations and directions of venting spent air.

3.1 Effect of Reynolds and Rayleigh numbers

The effects of the Reynolds number (Re) and the Rayleigh number (Ra) on Nusselt number (Nu) for different orientation of the hot surfaces is shown in Figs. 4 and 5 for maximum and minimum cross flows, respectively. Figures 4 and 5 show that, for all hot surface orientations and at any Ra, Nu increases with increasing Re for both cases of air ventings; venting with maximum or minimum cross flow. This can be attributed to the increase of the jet exit velocity with increasing the jet Reynolds number and this result in high level of turbulences at the stagnation zone, which yield to effective cooling of the surface. Increasing Reynolds number also increases the momentum of the flow which leads to higher heat removal rate. It appears from Figs. 4 and 5 that the average Nusselt follows a $Nu = C$

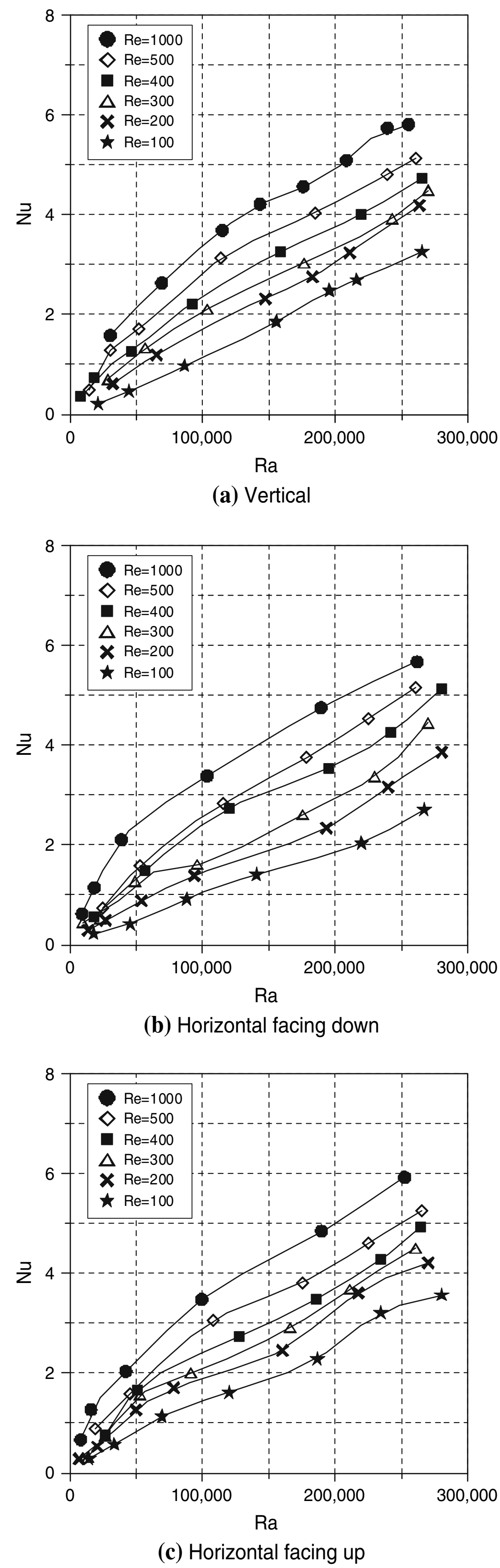

Fig. 4 Effect of Reynolds number, maximum cross flow

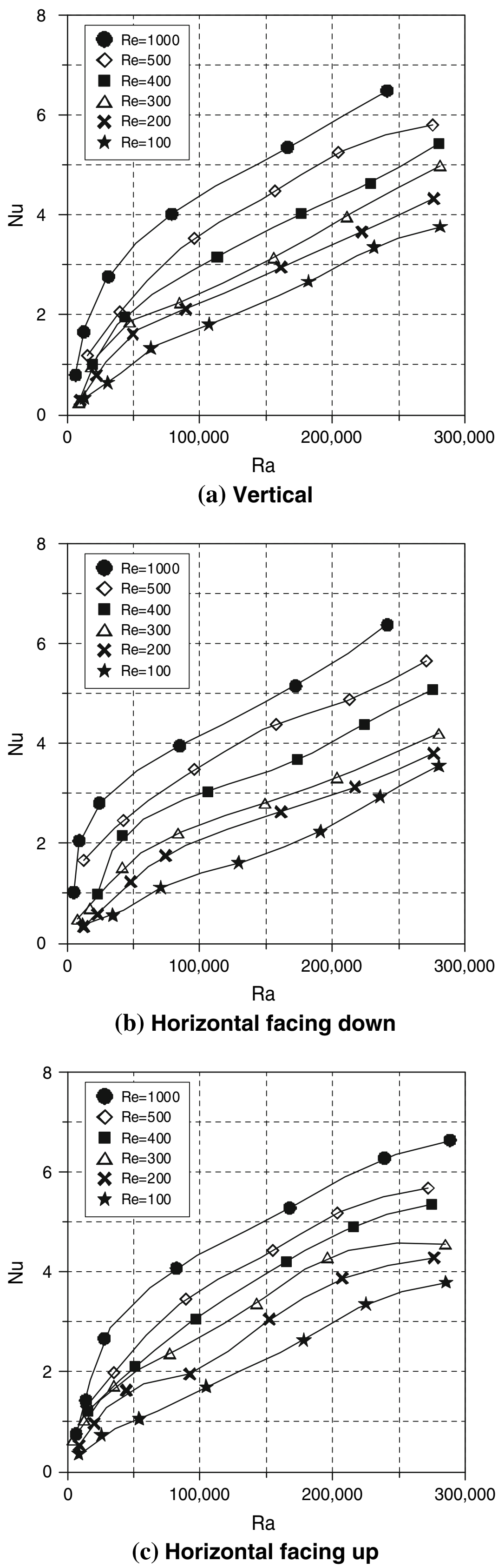

Fig. 5 Effect of Reynolds number, minimum cross flow

Re^m relationship. The constants of this relationship C and m seem to be dependent on Ra, hot surface orientation and strength of cross flow. As an example the data presented in Fig. 5a generate the $Nu = C\ Re^m$ correlations with the constants (C and m) equal (0.83, 0.46), (1.4, 0.42), (4.6, 0.3) at $Ra = 50{,}000$, 100,000 and 200,000, respectively. The variation of Re index from 0.42 to 0.3 due to the increase of Ra shows that the effect of Re on Nu becomes more dominant at lower value of Ra. The Re index in Nu correlation is close to the general Re index (about 0.5) for impinging jet without buoyancy effect.

Figures 4 and 5 show that for any Re and cross flow schemes and at the different hot surface orientations, the average Nusselt number generally increases with increasing Ra. This can be attributed to the increase of the buoyancy force with increasing Ra. Increasing buoyancy force increases flow driving force in the vertical direction and in consequently causes an increase of flow intensity in that direction. This either increases the intensity of the original flow (spent jet flow) or/and increase the turbulence level in the spent jet flow. Both effects lead to higher heat transfer rate. Also, increasing Ra enhances the mixing within the air layer due to the increase of turbulence and this leads to better heat transfer performance.

3.2 Effect of hot surface orientation

To clearly present and show the effect of the hot surface orientation on Nu, Figs. 4 and 5 are replotted in Figs. 6 and 7 with the hot surface orientation as a parameter for the two cases of cross flow schemes. As shown in Figs. 6 and 7, the dependence of Nu on the hot surface orientation varies according to Re and Ra ranges as follows:

(i) For $400 \le Re \le 1{,}000$ and at the entire range of Ra (10,000–280,000), Figs. 6a–c and 7a–c show that Nu is independent on the hot surface orientation. These ranges of Re and Ra give Ri in the range (0.0142–1.59). This means that, in these ranges of Re, Ra and Ri the buoyancy force is not dominant and the dominant force is the inertia/viscous forces. This means that, the strength of the buoyancy driven flow is small to affect of the inertia/viscous driven flow.

(ii) For $100 \le Re \le 300$ and $Ra \ge 10{,}000$ (these ranges of Re and Ra give $1.59 \le Ri \le 42.85$), Figs. 6d–f and 7d–f show that Nu depends on the orientation of the hot surface. These figures show that the Nu for horizontal orientation with hot surface facing down is less than that of vertical orientation surface and that of horizontal orientation with hot surface facing up. This means that in these ranges of Re and Ra, the buoyancy force is dominant and the strength of the buoyancy driven flow is able to affect the inertia/viscous driven flow. In case of horizontal orientation with hot

Fig. 6 Effect of orientation, maximum cross flow

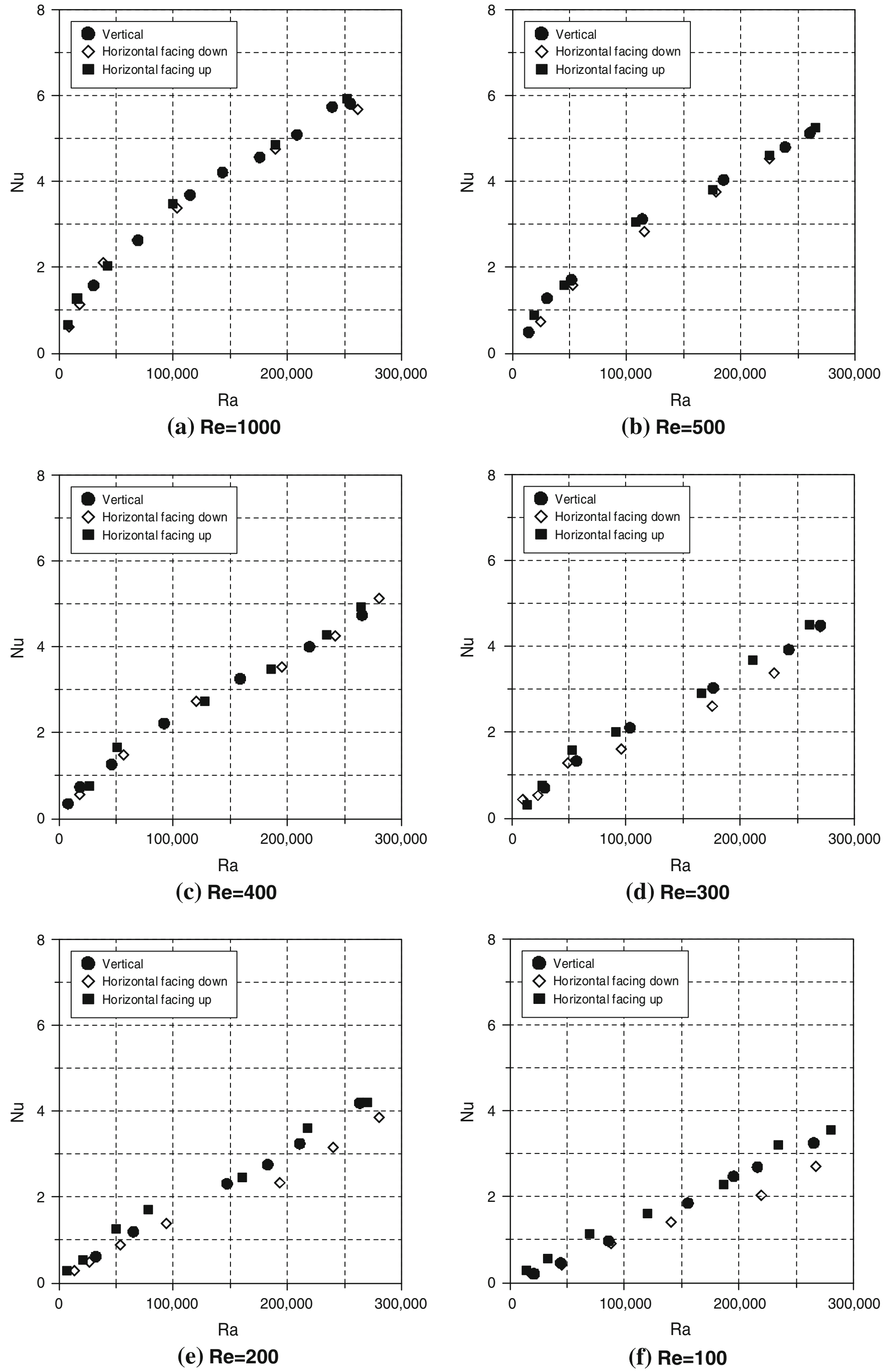

surface facing down, the buoyancy force (upwards) retard the air to flow away from the surface and this reduces the heat removal rate and *Nu* as compared to those of vertical orientation and for horizontal orientation with hot surface facing up. Considering the experimental uncertainties, Figs. 6d–f and 7d–f reveal that the Nusselt number for horizontal orientation with hot surface facing up is approximately equal to that of vertical orientation.

It can be concluded that the hot surface orientation in the case of cooling it by laminar air jets is important for

Fig. 7 Effect of orientation, minimum cross flow

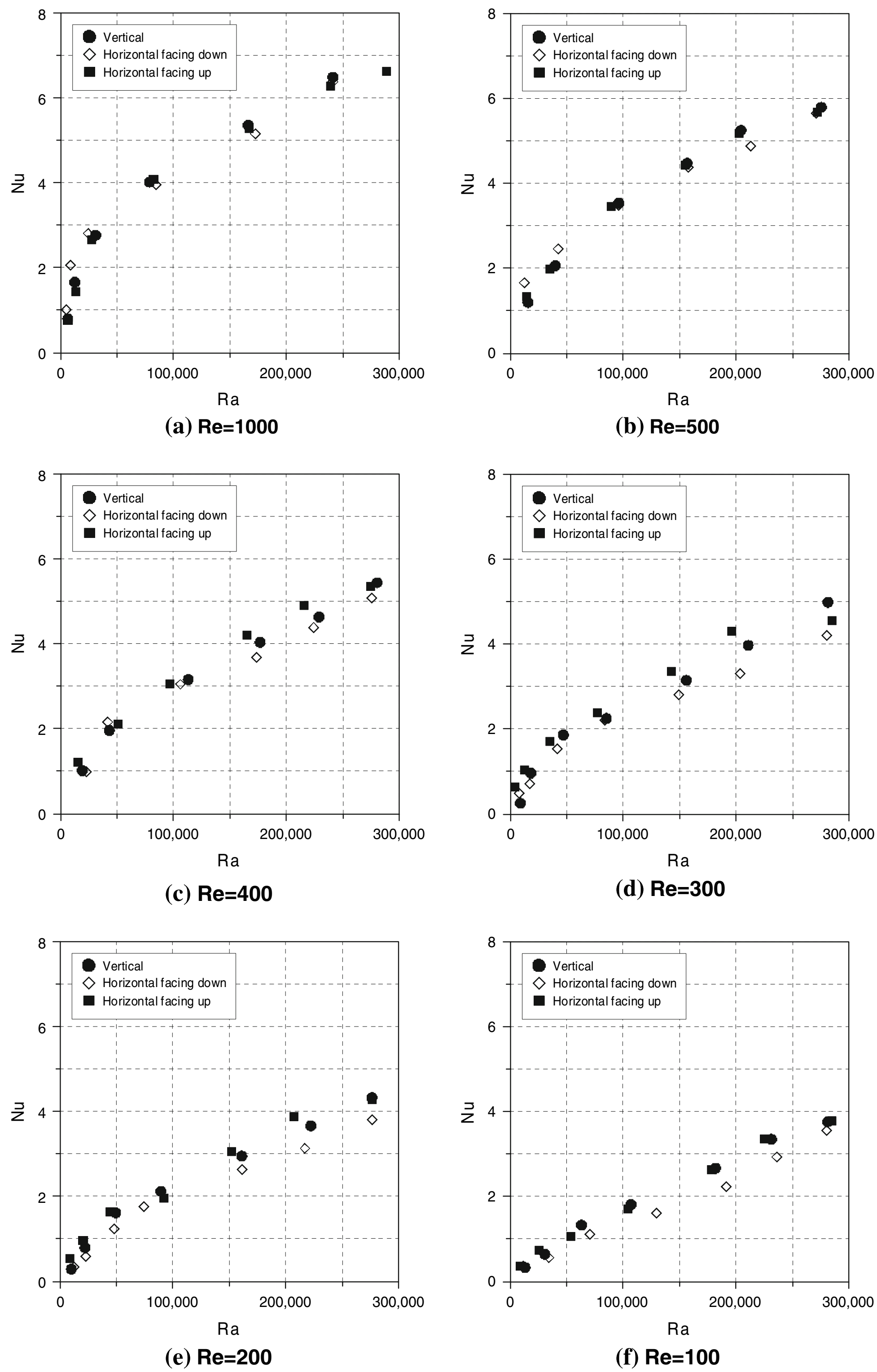

optimum performance in practical applications. The target hot surface is not preferable to be oriented horizontal with the hot surface facing down.

Figures 6 and 7 reveal that in the studied ranges of *Ra* and *Re* which give *Ri* in the range ($0.0142 \leq Ri \leq 42.85$) both forced and natural convection affects the total rate of heat transfer. This means that the resulting heat transfer mode falls in the mixed convection region. Figures 6 and 7 show that: (i) the forced convection mode is dominant if $0.0142 \leq Ri \leq 1.59$ whereas the direction of the buoyancy

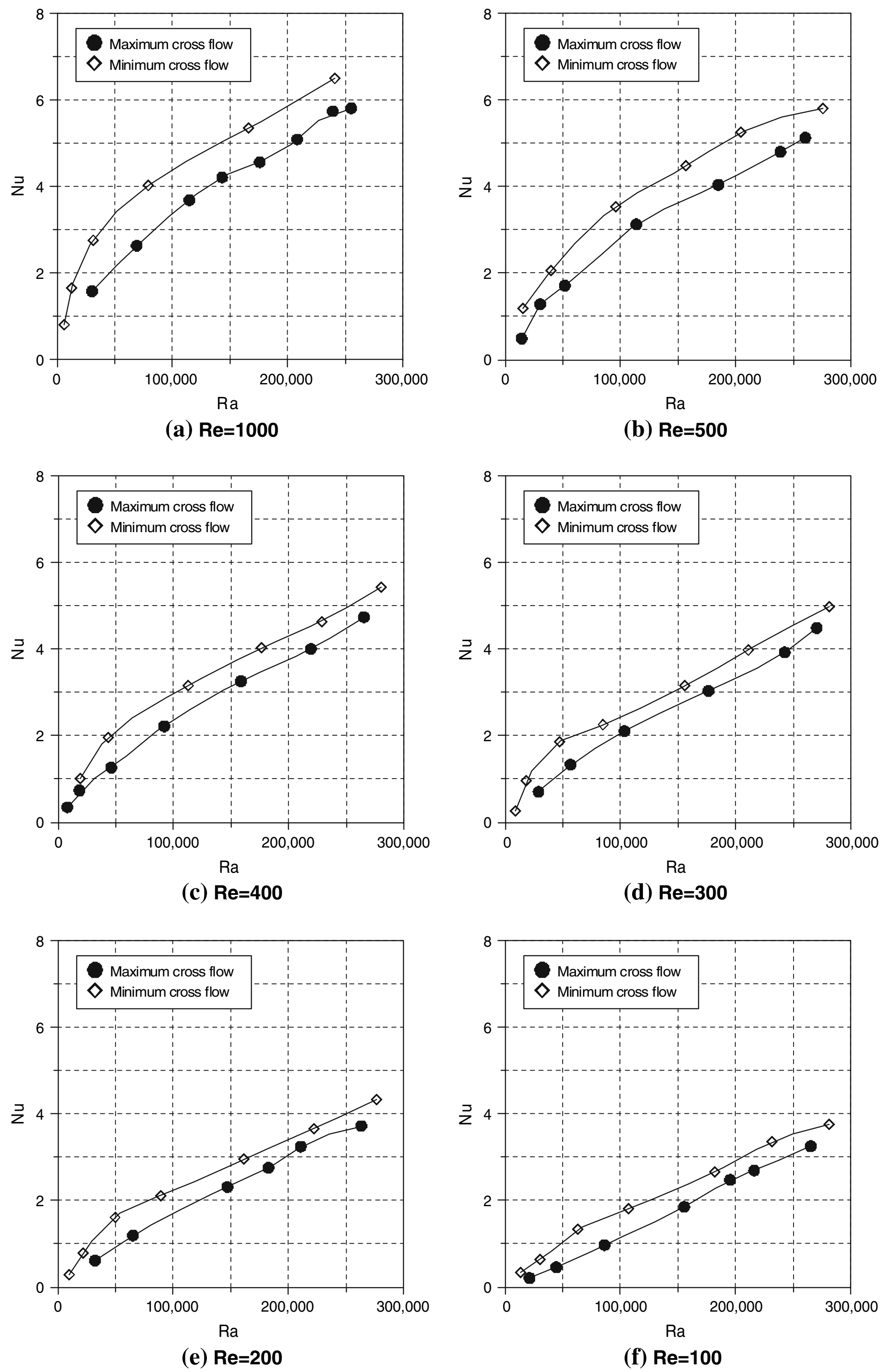

Fig. 8 Effect of cross flow, vertical hot surface

force can not affect the inertia/viscous force effect as shown in Figs. 6 and 7a–c, and (ii) the natural convection mode is dominant if $1.59 \le Ri \le 42.85$ where the direction of the buoyancy force can affect the inertia/viscous force effect as shown in Figs. 6 and 7d–f.

3.3 Effect of cross flow

Figures 8, 9, 10 show the effect of the cross flow schemes on Nu for Re = 1000, 500, 400, 300, 200 and 100 and at the entire range of Ra for vertical orientation and

Fig. 9 Effect of cross flow, horizontal facing down hot surface

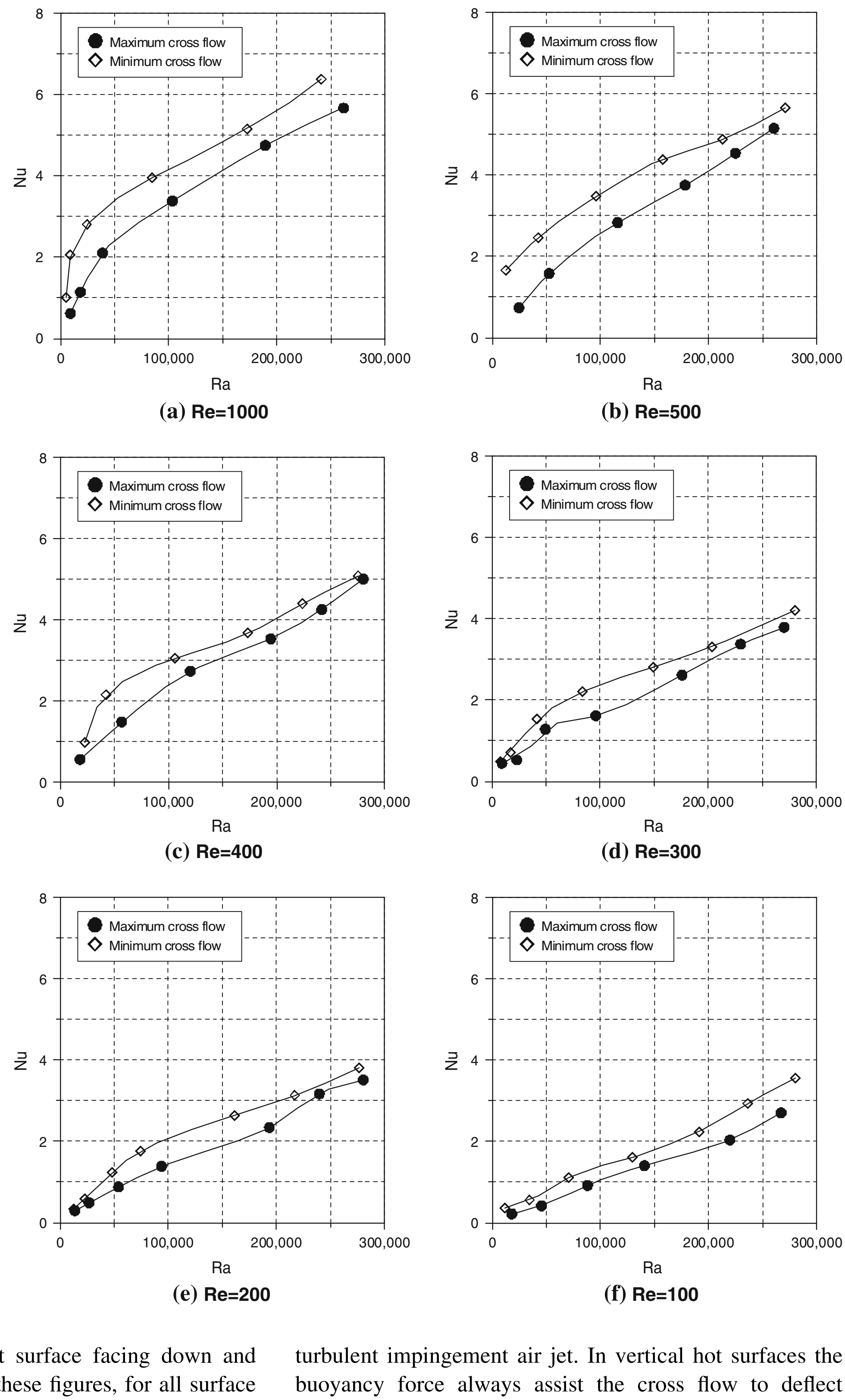

horizontal orientation with hot surface facing down and up, respectively. As shown in these figures, for all surface orientations and at the entire ranges of *Re* and *Ra*, the heat transfer rate with minimum cross flow is always higher than that of maximum cross flow. This behavior agrees with the behavior of the cross flow effect in turbulent impingement air jet. In vertical hot surfaces the buoyancy force always assist the cross flow to deflect the air jet and this reduces the local Nusselt number at the impingement point which leads to smaller average Nusselt number along the surface. In the case of horizontal orientation with hot surface facing up the buoyancy force

Fig. 10 Effect of cross flow, horizontal facing up hot surface

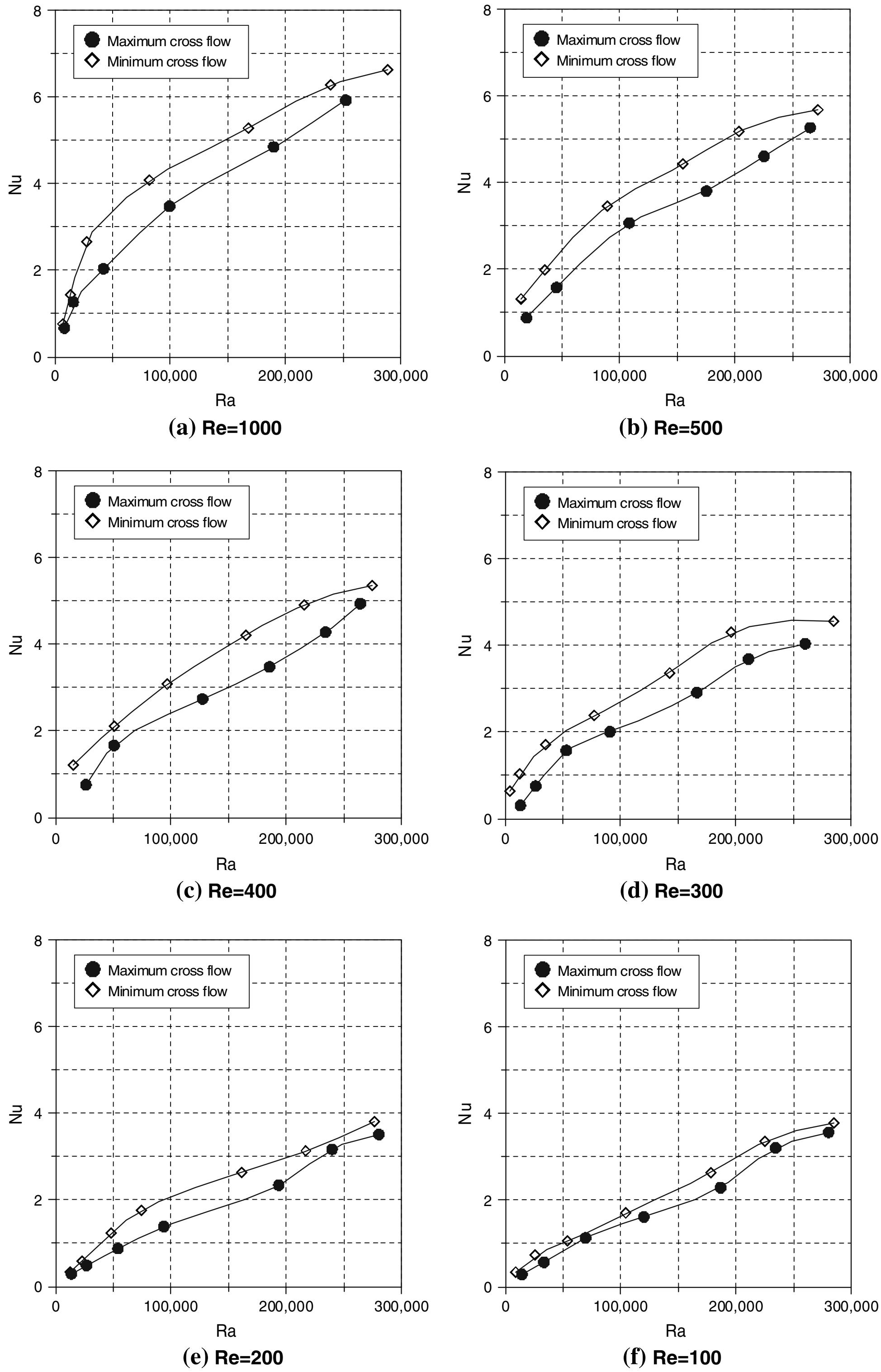

tends to move the air upwards and this leads to the formation of a resistance to the incoming air jet flow. This resistance reduces the strength of the air jet and makes it easy to be deflected by the cross flow and this leads to smaller heat transfer rate at the impingement point. In horizontal orientation with hot surface facing down the buoyancy force assists the hot flow to move up until it collides with the hot surface and then moves horizontally along the surface. This horizontal movement assists the cross flow to deflect the impingement jet at the impingement point and this reduces the local heat transfer at this point.

The discussion in the above section reveals that in laminar multiple air jets and for the different hot surface orientations, the buoyancy force always assists the cross flow on the decrease of the local heat transfer rate at the impingement points.

4 Comparison with literature

Numerical comparison of the present work with literature can not be conducted. The reason is that, for the author knowledge', no previous work was conducted to study the interaction of the effects of *Re, Ra, Ri,* orientation of the target hot surface and direction of spent air venting on heat transfer characteristics from a target hot surface cooled by impingement slot air jets array. In addition to that previous works that were conducted to study the effects of some of these parameters without including the effects of the other parameters were carried out at boundary conditions, geometrical conditions, and venting arrangements different from those used in this study. It was possible, however, to compare the trend of the results of the present work with those in the literature who separately study the effects of these parameters on the heat transfer characteristics. The present results agrees with the results of previous studies of jets in cross flow [9–14] where both works showed that cross flow always results in a decrease of heat transfer rate. Also, the present results agrees with the results of Rady [21] for a semi-confined laminar single slot jet impinging on an isothermal wall where both results concluded that, Nusselt number for upward facing hot surface (buoyancy assisted) is higher than the Nusselt number for downward facing hot surface (buoyancy retarded). Moreover both results showed the increase of the Nusselt number with the increase of the Richardson and Reynolds.

5 Summary and conclusions

An experimental work was conducted to study the effects of *Re, Ra, Ri,* orientation of the target hot surface and direction of spent air venting on heat transfer characteristics from a target hot surface cooled by impingement slot air jets array. The work also aimed to study the interaction of buoyancy effect, cross flow effect, and vortices formation effect on each other. The results showed that: (i) for the different cross flow schemes and at the different hot surface orientations, the average Nusselt number generally increases with increasing *Re* and *Ra*, (ii) the hot surface orientation in the case of cooling it by laminar air jets is important for optimum performance in practical applications; the target hot surface is not preferable to be oriented horizontal with the hot surface facing down, (iii) for $Re \geq 400$ and $Ra \geq 10{,}000$ (these ranges give $0.0142 \leq Ri \leq 1.59$) the Nusselt number is independent on the hot surface orientation, (iv) and for $Re \leq 300$ and $Ra \geq 100{,}000$ (these ranges give $1.59 \leq Ri \leq 42.85$) the Nusselt number of horizontal orientation with hot surface facing down is less than that of vertical orientation and that of horizontal orientation with hot surface facing up and the Nusselt number of vertical orientation is approximately equal to that of horizontal orientation with hot surface facing up, (v) for all surfaces orientations and at all ranges of *Re* and *Ra*, increasing the strength of the cross flow decreases the effective cooling of the surface, (vi) the forced convection mode was dominant if $0.0142 \leq Ri \leq 1.59$ and the natural convection mode was dominant if $1.59 \leq Ri \leq 42.85$, and (vii) in laminar multiple air jets and for the different hot surface orientations, the buoyancy force always assists the cross flow on the decrease of the local heat transfer rate at the impingement points.

References

1. Sezai I, Aldabbagh LBY (2003) The effect of jet-to-jet spacing on the cooling performance of impinging jet arrays. In: Proceedings of 31CCHMT, 3rd international conference on computational heat and mass transfer, Banff, Canada 26–30
2. Sezai I, Aldabbagh LBY (2004) A three dimensional numerical investigation of flow and heat transfer characteristics of inline jet arrays. Numr Heat Transfer 45:271–288
3. Kelso RM, Smith AJ (1995) Horseshow vortex systems resulting from the interaction between a laminar boundary layer and a transfer jet. Phys Fluids 7:153–158
4. Fric TF, Rosshko A (1994) Vortical Structure of the near field of the transverse jet. J Fluid Mech 1–47
5. Kelso RM, Lim TT, Perry AE (1996) An experimental study of round jets in cross-flow. J Fluid Mech 306:111–114
6. Barata JMM (1996) Fountain flows produced by multiple impingement jets in a cross-flow. AAIA J 34(12):2523–2530
7. Kim SW, Benson TJ (1993) Fluid flow of a row of jets in cross flow. A numerical study. AIAA J 31(5):806–811
8. Aldabbagh LBY, Mohamed AA (2006) Effect of jet to plate spacing in laminar array jets impinging. Heat Mass Transfer 43(3):265–273
9. Goldstein RJ, Behbahani AI (1982) Impingement of a circular jet with and without cross flow. Int J Heat and Mass Transfer 25(10):1377–1382
10. Al-Sanea S (1992) A numerical study of the flow and heat transfer characteristics of an impinging laminar slot jet including cross flow effect. Int J Heat Mass Transfer 35(10):2502–2513
11. Metzger DE, Florshuetz LW, Takeuchi DI, Bhee RD, Berry RA (1979) Heat transfer characteristics for inline and staggered arrays of circular jets with cross-flow of spent air. J Heat Transfer 101:526–531
12. Florshuetz LW, Berry RA, Metzger DE (1980) Periodic streamwise variations of heat transfer coefficients for inline and staggered arrays of circular jets with cross flow of spent air. ASME J Heat Transfer 102:132–137
13. Yoon PH, Rhee DH, Cho HH (2000) Effects of arrays of impinging jets with cross flow on heat/mass transfer. KEME J B 4(2):195–203

14. Kanokjaruvijit K, Martinez-boats RF (2005) Jet impingement on a dimpled surface with different cross flow schemes. Int J Heat Mass Transfer 48:161–170
15. Yang YT, Wang YX (2005) Three-dimensional numerical simulation of an inclined jet with cross-flow. Int J Heat Mass Transfer 48:4019–4027
16. Aldabbagh LBY, Sezai I, Mohamad AA (2003) Three dimensional investigation of a laminar impinging square jet interaction with cross flow. J Heat Transfer ASME 125:243–249
17. Rady M, Arquis E (2006) Heat transfer enhancement of multiple impinging slot jets with symmetric exhaust ports and confined surface protrusions. Appl Therm Eng 26:1310–1319
18. Satyanarayana S, Jaluria Y (1982) A study of laminar buoyancy jets discharged at an inclination to the vertical buoyancy force. Int J Heat Mass Transfer 25:1569–1577
19. Yan TD, Liburdy JA, Wg T (1988) Buoyancy effects on laminar impingining jets. Int J Heat Mass Transfer 31:2137–2145
20. Sahoo D, Sharif MAR (2004) Numerical modeling of slot-jet impingement cooling of a constant heat flux surface confined by a parallel wall. Int J Thermal Sci 43:877–887
21. Rady MA (2000) Buoyancy effects on the flow and heat transfer characteristics of an impinging semi-confined slot jet. Int J Trans Phenomena 2:113–126
22. Incropera FP, DeWitt DP (1995) Introduction to heat transfer. Wiley, New York
23. Suryanarayana NV (1995) Engineering heat transfer. West Publishing Company, New York
24. Holman JP, Gajda WJ (1989) Experimental method for engineers. McGraw Hill, New York